Optomechanical Bell Test

Marinković, Igor; Wallucks, Andreas; Riedinger, Ralf; Hong, Sungkun; Aspelmeyer, Markus; Gröblacher, Simon

DOI
10.1103/PhysRevLett.121.220404

Publication date
2018

Document Version
Final published version

Published in
Physical Review Letters

Editors' Suggestion | Featured in Physics

Optomechanical Bell Test

Igor Marinković,[1,*] Andreas Wallucks,[1,*] Ralf Riedinger,[2] Sungkun Hong,[2] Markus Aspelmeyer,[2] and Simon Gröblacher[1,†]
[1]*Department of Quantum Nanoscience, Kavli Institute of Nanoscience, Delft University of Technology, 2628CJ Delft, Netherlands*
[2]*Vienna Center for Quantum Science and Technology (VCQ), Faculty of Physics, University of Vienna, A-1090 Vienna, Austria*

(Received 18 June 2018; published 29 November 2018)

Over the past few decades, experimental tests of Bell-type inequalities have been at the forefront of understanding quantum mechanics and its implications. These strong bounds on specific measurements on a physical system originate from some of the most fundamental concepts of classical physics—in particular that properties of an object are well-defined independent of measurements (realism) and only affected by local interactions (locality). The violation of these bounds unambiguously shows that the measured system does not behave classically, void of any assumption on the validity of quantum theory. It has also found applications in quantum technologies for certifying the suitability of devices for generating quantum randomness, distributing secret keys and for quantum computing. Here we report on the violation of a Bell inequality involving a massive, macroscopic mechanical system. We create light-matter entanglement between the vibrational motion of two silicon optomechanical oscillators, each comprising approx. 10^{10} atoms, and two optical modes. This state allows us to violate a Bell inequality by more than 4 standard deviations, directly confirming the nonclassical behavior of our optomechanical system under the fair sampling assumption.

DOI: 10.1103/PhysRevLett.121.220404

Bell's theorem [1] predicts that any local realistic theory is at variance with quantum mechanics. It was originally conceived to settle an argument between Einstein [2] and Bohr [3] on locality in physics, and to investigate the axioms of quantum physics. First tests of the Clauser-Horne-Shimony-Holt (CHSH) inequality [4], an experimentally testable version of Bell's original inequality, were performed with photons from cascaded decays of atoms [5,6] and parametric down-conversion [7–9]. Subsequent experiments reduced the set of assumptions required for the falsification of classical theories, closing, e.g., the locality [10] and detection loopholes [11], first individually and recently simultaneously [12–15]. In addition to the fundamental importance of these experiments, the violation of a Bell-type inequality has very practical implications—in particular, it has become the most important benchmark for thrust-worthily verifying entanglement in various systems [16,17], including mesoscopic superconducting circuits [18], for certifying randomness [19,20], secret keys [21], and quantum computing [22].

While the standard form of quantum theory does not impose any limits on the mass or size of a quantum system [23], the potential persistence of quantum effects on a macroscopic scale seems to contradict the human experience of classical physics. Over the past years, quantum optomechanics has emerged as a new research field, coupling mechanical oscillators to optical fields. While these systems are very promising for quantum information applications due to their complete engineerability, they also hold great potential to test quantum physics on a new mass scale. Recent experiments have demonstrated quantum control of such mechanical systems, including mechanical squeezing [24], single-phonon manipulation [25–28], as well as entanglement between light and mechanics [29] and entanglement between two mechanical modes [30–32]. However, explaining the observed results in these experiments required assuming the validity of quantum theory at some level. A Bell test, in contrast, is a genuine test of nonclassicality without quantum assumptions.

Here we report on the first Bell test using correlations between light and microfabricated mechanical resonators, which constitute massive macroscopic objects, hence verifying nonclassical behavior of our system without relying on the quantum formalism. Bell tests do not require assumptions about the physical implementation of a quantum system such as the dimension of the underlying Hilbert space or the fundamental interactions involved in state preparation and measurement [33]. The violation of a Bell inequality is hence the most unambiguous demonstration of entanglement with numerous important implications. From a fundamental perspective, the robust entanglement between flying optical photons and a stored mechanical state rules out local hidden variables, which can be used for further tests of quantum mechanics at even larger mass scales [34,35]. From an application perspective, the presented measurements also imply that optomechanics is a promising technique to be used for quantum information processing tasks including teleportation, quantum memories, and the possibility of quantum communication with device-independent security [21].

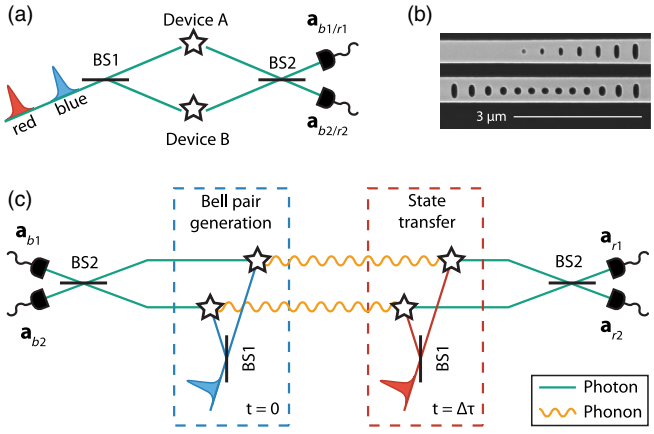

FIG. 1. (a) Schematic of the setup: blue detuned drive pulses interact with the mechanical resonators (devices A and B) producing entangled photon-phonon pairs. The light-matter entanglement is in the path basis (A or B), corresponding to the device in which the Stokes scattering event took place. The generated photons are detected in single-photon detectors giving the measurement results a_{b1} and a_{b2}. The detection of the phonons is done by transferring their states to another optical mode by using a red drive after some time $\Delta\tau$ and, subsequently, obtaining the results a_{r1} and a_{r2}. Note that for technical reasons the photons created by the blue and red drives are detected on the same pair of detectors, but with a time delay $\Delta\tau = 200$ ns. Therefore we have time separation of the two parties of the Bell test instead of space separation (as commonly done). BS1/2 represent beam splitter 1/2. (b) Scanning electron microscope image of one of the optomechanical devices, represented with a star symbol in (a) and (c), next to the coupling waveguide (top). (c) Illustration of our experimental sequence: one party of the Bell test measures in which detector path the Stokes photon is found at time $t = 0$, while the other performs the same measurement for the anti-Stokes photon after a time $t = \Delta\tau$. We probe their correlations in order to violate the CHSH inequality. Since the two photons never interacted directly (only through the mechanics), the observed correlations are a direct consequence of the correlations between the Stokes photons and phonons.

The optomechanical structures used in this work are two photonic crystal nanobeams on two separate chips. They are designed to have an optical resonance in the telecom band that is coupled to a colocalized, high-frequency mechanical mode [36]. Each device is placed in one of the arms of an actively stabilized fiber interferometer (see Ref. [31] and the Supplemental Material [37] for additional details). The resonators are cryogenically cooled close to their motional ground state inside a dilution refrigerator. Our entanglement creation and verification protocol consists of two optical control pulses that give rise to linearized optomechanical interactions, addressing the Stokes and anti-Stokes transitions of the system (see Fig. 1). Both types of interactions result in scattered photons that are resonant with the cavity and can be efficiently filtered from the drive beams before being detected by superconducting nanowire single photon detectors (SNSPDs).

A blue detuned, ~40 ns long laser pulse with frequency $\nu_b = \nu_o + \nu_m$ (ν_o optical resonance, ν_m mechanical resonance) generates photon-phonon pairs. The interaction in this case is described by $\hat{H}_b = -\hbar g_0 \sqrt{n_b}\hat{a}^\dagger \hat{b}^\dagger + \text{H.c.}$, with the intracavity photon number n_b, the optomechanical single photon coupling g_0 and the optical (mechanical) creation operators $\hat{a}^\dagger$ ($\hat{b}^\dagger$). This correlates the number of mechanical and optical excitations in each of the arms of the interferometer as

$$|\psi\rangle \propto [|00\rangle_{om} + \epsilon|11\rangle_{om} + \mathcal{O}(\epsilon^2)], \tag{1}$$

where o denotes the optical and m the mechanical mode, while $p = \epsilon^2$ is the excitation probability. For small $p \ll 1$, states with multiple excitations are unlikely to occur, and can therefore be neglected in the statistical analysis. Driving the devices simultaneously and postselecting on trials with a successful detection of both the Stokes photon and the phonon, we approximate the combined state as

$$\begin{aligned}|\Psi\rangle &= \frac{1}{\sqrt{2}}(|11\rangle_A|00\rangle_B + e^{i\phi_b}|00\rangle_A|11\rangle_B) \\ &= \frac{1}{\sqrt{2}}(|AA\rangle_{om} + e^{i\phi_b}|BB\rangle_{om}),\end{aligned} \tag{2}$$

again neglecting higher order excitations. Here ϕ_b is the phase difference that the blue drives acquire in the two interferometer paths A and B, including the phase shift of the first beam splitter. Expressing the state in a path basis $|A\rangle_x = |10\rangle_{AB}$, where x is o for the photonic and m for the phononic subsystem in arms A and B, allows us to identify the Bell state, similarly to polarization entanglement in optical down-conversion experiments. Unlike the two mode entangled mechanical state in Ref. [31], this four-mode entangled optomechanical state allows us to realize a Bell measurement of the type suggested by Horne, Shimony, and Zeilinger [39] and first demonstrated by Rarity and Tapster [8] involving two-particle interference between four different modes. In order to access interferences between the mechanical modes, we convert the phonons into photons using a red-detuned laser pulse (duration ~40 ns, drive frequency $\nu_r = \nu_o - \nu_m$). This realizes an optomechanical beam splitter interaction which allows for a state transfer ($\hat{H}_r = -\hbar g_0 \sqrt{n_r}\hat{a}^\dagger \hat{b} + \text{H.c.}$, with the intracavity photon number n_r). Note that this can also be described as a classical mapping process. The optical readout fields in the interferometer arms are again recombined on a beam splitter, after which the state of Stokes or anti-Stokes field is

$$\begin{aligned}|\Phi\rangle = \frac{1}{2\sqrt{2}}[&(1 - e^{i(\phi_b+\phi_r)})(\hat{a}^\dagger_{r1}\hat{a}^\dagger_{b1} - \hat{a}^\dagger_{r2}\hat{a}^\dagger_{b2}) \\ &+ i(1 + e^{i(\phi_b+\phi_r)})(\hat{a}^\dagger_{r1}\hat{a}^\dagger_{b2} + \hat{a}^\dagger_{r2}\hat{a}^\dagger_{b1})]|0000\rangle.\end{aligned} \tag{3}$$

Here we express the detected fields in terms of their creation operators with labels b (r) for photons scattered

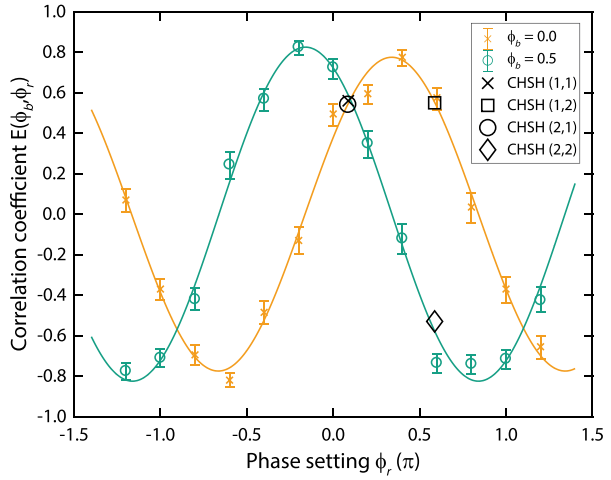

FIG. 2. Correlation coefficients for various phase settings. We set the blue phase parameter ϕ_b to 0 (orange) and 0.5π (green), while we scan the red pulse's phase setting ϕ_r over more than 2π. The optimal angles to test the CHSH inequality are shown with different symbols. The associated measured values can be found in Table I.

from the blue (red) drive and 1 (2) for the two detectors (cf. Fig. 1). Furthermore ϕ_r is the phase difference that the red detuned pulse photons acquire in the two arms of the interferometer. Since experimentally the mechanical frequencies of the devices differ by a small offset $\Delta\nu_m$ (see below), the state acquires an additional phase $\Omega = \Delta\nu_m \Delta\tau$, where $\Delta\tau$ is the delay between the blue and red pulses. In all data below, however, we keep $\Delta\tau$ fixed such that we can treat it as constant and set $\Omega = 0$. Typically, Bell experiments are done by rotating the measurement basis in which each particle is detected. Equivalently, the state itself can be rotated, while keeping the measurement basis fixed. In our experiment we choose the latter option, as this is simpler to implement in our setup. We achieve this by applying a phase shift with an electro-optical modulator (EOM) in arm A of the interferometer, with which we can vary ϕ_b and ϕ_r independently (see Supplemental Material [37]). This allows us to select the relative angles between the photonic and phononic states.

In our experiment, the optical resonances are at a wavelength of $\lambda = 1550.4$ nm with a relative mismatch of $\Delta\nu_o \approx 150$ MHz. The mechanical modes have frequencies of $\nu_m = 5.101$ and 5.099 GHz for device A and B, respectively. The bare optomechanical coupling rate $g_0/2\pi$ is 910 kHz for device A and 950 kHz for device B. While the optical mismatch is much smaller than the linewidth $\Delta\nu_o \ll \kappa \sim 1$ GHz such that the devices are sufficiently identical, the mechanical mismatch requires optical compensation. This is realized using the EOM in arm A of the interferometer to ensure that the scattered photons from each arm interfere with a well-defined phase on the second beam splitter (see also Supplemental Material [37]).

At the base temperature of the dilution refrigerator of around 12 mK we obtain the phonon temperature of the mechanical modes by performing sideband asymmetry measurements [40]. The measured thermal occupations for both devices is $n_{\mathrm{init}} \leq 0.09$. We determine the lifetimes of the phonons in our structures to be $\tau_A = 3.3 \pm 0.5$ μs and $\tau_B = 3.6 \pm 0.7$ μs using a pump-probe type experiment in which we excite the devices and vary the delay to the readout pulse. To reinitialize the devices in their ground states prior to each measurement trial, we repeat the drive sequence every 50 μs, leaving more than 10 times their lifetime for thermalization with the environment. Furthermore, we set the delay between the blue and red detuned pulses to $\Delta\tau = 200$ ns. The pulse energies for the Bell inequality experiment are chosen such that the excitation probability is 0.8% (1%), while the readout efficiency is 3% (4.1%) for device A (device B). These probabilities match the number of optomechanically generated photons for each device at the beam splitter.

To characterize the performance of the devices, we first perform cross-correlation measurements of the photons scattered from blue and red drives on each individual optomechanical system. With the above-mentioned settings, we obtain normalized cross-correlation values of $g^{(2)}_{br,A} = 9.3 \pm 0.5$ and $g^{(2)}_{br,B} = 11.2 \pm 0.6$ [40]. We can use this to estimate the expected interferometric visibility for the experiments below as $V_{\mathrm{xpcd}} = [g^{(2)}_{br} - 1]/[g^{(2)}_{br} + 1]$ [41]. As there is a small mismatch in the observed cross-correlations of the two devices, we use the smaller value of device A, which results in an expected visibility of around $V_{\mathrm{xpcd}} = 81\%$.

In order to experimentally test a Bell inequality, we then drive the two devices simultaneously in a Mach-Zehnder interferometer (see Fig. 1 and the Supplemental Material [37]). We define the correlation coefficients

$$E(\phi_b, \phi_r) = \frac{n_{11} + n_{22} - n_{12} - n_{21}}{n_{11} + n_{22} + n_{12} + n_{21}}. \tag{4}$$

Here n_{ij} represents the number of detected coincidences scattered from blue (i) and red (j) pulses on the two detectors ($i, j = 1, 2$), such that, e.g., n_{21} is the number of trials where the blue drive resulted in an event on detector 2, whereas the consecutive red drive on detector 1. The visibility V is given as the maximum correlation coefficient $V = |E(\phi_b, \phi_r)|_{\max}$. We measure the correlation coefficients for various phase settings for the blue (ϕ_b) and red (ϕ_r) pulses, as shown in Fig. 2. Strong correlations in the detection events by photons scattered from blue and red pump pulses can be seen, of which the latter are a coherent mapping of the mechanical state of the resonator. This sweep demonstrates that we are able to independently shift the phases for the Stokes and anti-Stokes states. The visibility $V = 80.0 \pm 2.5\%$ we obtain from fitting the data matches the prediction from the individual

TABLE I. Correlation coefficients for the optimal CHSH angles. The violation of the inequality can be computed according to Eq. (5) and results in a S value of $S = 2.174^{+0.041}_{-0.042}$, corresponding to a violation of the classical bound by more than 4 standard deviations.

Settings i, j	$\phi_b^i[\pi]$	$\phi_r^j[\pi]$	$E(\phi_b, \phi_r)$
(1,1)	0.0	0.087	$0.561^{+0.019}_{-0.020}$
(1,2)	0.0	0.587	$0.550^{+0.020}_{-0.022}$
(2,1)	0.5	0.087	$0.542^{+0.018}_{-0.021}$
(2,2)	0.5	0.587	$-0.523^{+0.021}_{-0.021}$

cross-correlation measurements very well. The interference furthermore shows the expected periodicity of 2π.

To test possible local hidden-variable descriptions of our correlation measurements we use the CHSH inequality [4], a Bell-type inequality. Using the correlation coefficients $E(\phi_b, \phi_r)$, it is defined as

$$S = |E(\phi_b^1, \phi_r^1) + E(\phi_b^1, \phi_r^2) + E(\phi_b^2, \phi_r^1) - E(\phi_b^2, \phi_r^2)| \leq 2. \tag{5}$$

A violation of this bound allows us to exclude a potential local realistic theory from describing the optomechanical state that we generate in our setup. The maximal violation $S_{\mathrm{QM}} = 2\sqrt{2}V$ is expected for settings $\phi_b^i = [0, \pi/2]$ and $\phi_r^j = [-\pi/4 + \phi_c, \pi/4 + \phi_c]$, with $i, j = 1, 2$ [42]. Here $\phi_c = 0.337\pi$ is an arbitrary, fixed phase offset that is inherent to the setup. Our experimentally achieved visibility exceeds the minimal requirement for a violation of the classical bound $V \geq 1/\sqrt{2} \approx 70.7\%$. We proceed to directly measure the correlation coefficients in the four settings, as indicated in Fig. 2, and obtain $S = 2.174^{+0.041}_{-0.042}$ (cf. Table I). This corresponds to a violation of the CHSH inequality by more than 4 standard deviations, clearly confirming the nonclassical character of our state. From the observed visibility of $V = 80.0\%$, we would expect a slightly stronger violation with $S \approx 2.26$. The reduction in our experimentally obtained value for S can be attributed to imperfect filtering of drive photons in front of one of the SNPSDs, which gives rise to varying amounts of leak photons at different phase settings (see discussion in the Supplemental Material [37]).

For quantum network applications it is also important to analyze the quality of the detected optomechanical entanglement with regard to the detection rate. In our measurements we can achieve this by changing the energies of the drive beams to alter the optomechanical interaction strengths. An increase in the blue pulse energy is accompanied by two mechanisms that decrease the state fidelity. First, the probability for higher order scattering events $\mathcal{O}(p_{A,B}^2)$ is increased. Second, higher pulse energies also result in more absorption, degrading the state through

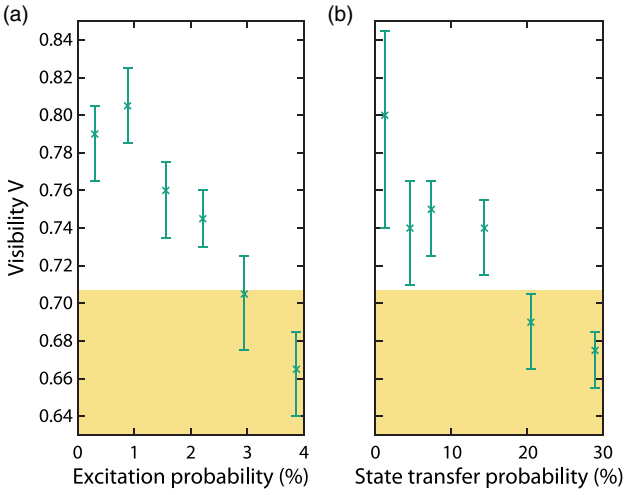

FIG. 3. Visibility as a function of generation rate and state transfer probability. We sweep the power of the blue pulse while keeping the red state transfer probability fixed, inducing absorption of the optical field in the silicon structure, and see that for excitation probabilities up to around 3% the measured visibility exceeds the threshold to violate the CHSH inequality (left). When increasing only the red pump power (right) a similar behavior can be observed, allowing us to increase the state transfer probability beyond 14%, while still being able to overcome the classical bound (orange shaded region). The visibilities $V = |E(\phi_b, \phi_r)|_{\max}$ are measured in a single phase setting at the optimal angles $\phi_b = 0$ and $\phi_r = 0.337\pi$.

thermal excitations. As observed in previous experiments [31,40], optical pumping of the devices creates a thermal population of the mechanical modes with timescales on the order of several hundreds of nanoseconds (see also the Supplemental Material [37]). While we keep the delay to the readout pulse short ($\Delta\tau = 200$ ns), we cannot fully avoid these spurious heating effects. Hence the decrease in visibility with increased pulse energy, as seen in Fig. 3(a), can be attributed mostly to this direct absorption heating. To further test the heating dynamics of our state, we also sweep the red pulse energies while keeping the excitation energy fixed at the value used in the main experiment ($p_b = 0.8\%$ and 1%). As expected, the increased readout pulse energies lead to substantial heating of the devices [27]. However, even for relatively large optical powers corresponding to ~14% readout efficiency, the correlation coefficient is above the threshold for violating a Bell inequality under the fair sampling assumption, see Fig. 3(b).

Our system is fully engineered and hence we have complete control over the resonance frequencies and possibilities to integrate with other systems. While in our current structures we intentionally cap the mechanical quality factors to keep the measurement time short [43], recent experiments with very similar devices have observed lifetimes larger than 1 s [44]. Long lived nonclassical states of large masses are interesting for fundamental studies of

quantum mechanics. Combined with the fact that we can efficiently couple these states to photons in the telecom band could enable interesting experiments with Bell tests at remote locations. Employing fast optical switches that route one of the photons to a second set of detectors would furthermore allow us to close the locality loophole in the future. Our probabilistic scheme could, in principle, also be adapted to perform a "loophole-free" Bell test [13], if in addition the detection loophole would be closed through a more efficient readout.

In summary, we have demonstrated the violation of a Bell-type inequality using massive (around 10^{10} atoms), macroscopic optomechanical devices, thereby verifying the nonclassicality of their state without the need for a quantum description of our experiment. The experimental scheme demonstrated here may also be employed in other, even more massive optomechanical systems. One outstanding challenge is to generate states of genuine macroscopic distinction, for example, a macroscopic separation in the center of mass, to investigate fundamental decoherence mechanisms [45] or even the interplay between quantum physics and gravity [46,47]. We also show that the created entangled states are relatively robust to absorption heating, which could lead to a realistic implementation of entanglement generation for a future quantum network using optomechanical devices. Violation of a CHSH inequality can also be used to verify long-distance quantum communication with device-independent security using mechanical systems.

We would like to thank Vikas Anant, Nicolas Sangouard, and Joshua Slater for valuable discussions and support. We also acknowledge assistance from the Kavli Nanolab Delft, in particular from Marc Zuiddam and Charles de Boer. This project was supported by the Foundation for Fundamental Research on Matter (FOM) Projectruimte grants (15PR3210, 16PR1054), the European Research Council (ERC StG Strong-Q, ERC CoG QLev4G), the European Commission under the Marie Curie Horizon 2020 initial training programme OMT (Grant No. 722923), the Vienna Science and Technology Fund WWTF (ICT12-049), the Austrian Science Fund (FWF) under Projects No. F40 (SFB FOQUS) and No. P28172, and by the Netherlands Organisation for Scientific Research (NWO/OCW), as part of the Frontiers of Nanoscience program, as well as through a Vidi grant (680-47-541/994). R. R. is supported by the FWF under Project No. W1210 (CoQuS) and is a recipient of a DOC fellowship of the Austrian Academy of Sciences at the University of Vienna.

*These authors contributed equally to this work.
†s.groeblacher@tudelft.nl

[1] J. S. Bell, Physics **1**, 195 (1964).
[2] A. Einstein, B. Podolsky, and N. Rosen, Phys. Rev. **47**, 777 (1935).
[3] N. Bohr, Phys. Rev. **48**, 696 (1935).
[4] J. F. Clauser, M. A. Horne, A. Shimony, and R. A. Holt, Phys. Rev. Lett. **23**, 880 (1969).
[5] S. J. Freedman and J. F. Clauser, Phys. Rev. Lett. **28**, 938 (1972).
[6] A. Aspect, P. Grangier, and G. Roger, Phys. Rev. Lett. **47**, 460 (1981).
[7] Y. H. Shih and C. O. Alley, Phys. Rev. Lett. **61**, 2921 (1988).
[8] J. G. Rarity and P. R. Tapster, Phys. Rev. Lett. **64**, 2495 (1990).
[9] P. G. Kwiat, K. Mattle, H. Weinfurter, A. Zeilinger, A. V. Sergienko, and Y. Shih, Phys. Rev. Lett. **75**, 4337 (1995).
[10] G. Weihs, T. Jennewein, C. Simon, H. Weinfurter, and A. Zeilinger, Phys. Rev. Lett. **81**, 5039 (1998).
[11] M. A. Rowe, D. Kielpinski, V. Meyer, C. A. Sackett, W. M. Itan, C. Monroe, and D. J. Wineland, Nature (London) **409**, 791 (2001).
[12] B. Hensen *et al.*, Nature (London) **526**, 682 (2015).
[13] M. Giustina *et al.*, Phys. Rev. Lett. **115**, 250401 (2015).
[14] L. K. Shalm *et al.*, Phys. Rev. Lett. **115**, 250402 (2015).
[15] W. Rosenfeld, D. Burchardt, R. Garthoff, K. Redeker, N. Ortegel, M. Rau, and H. Weinfurter, Phys. Rev. Lett. **119**, 010402 (2017).
[16] J. T. Barreiro, J.-D. Bancal, P. Schindler, D. Nigg, M. Hennrich, T. Monz, N. Gisin, and R. Blatt, Nat. Phys. **9**, 559 (2013).
[17] R. Schmied, J.-D. Bancal, B. Allard, M. Fadel, V. Scarani, P. Treutlein, and N. Sangouard, Science **352**, 441 (2016).
[18] M. Ansmann *et al.*, Nature (London) **461**, 504 (2009).
[19] S. Pironio *et al.*, Nature (London) **464**, 1021 (2010).
[20] P. Bierhorst *et al.*, Nature (London) **556**, 223 (2018).
[21] A. Acín, N. Brunner, N. Gisin, S. Massar, S. Pironio, and V. Scarani, Phys. Rev. Lett. **98**, 230501 (2007).
[22] P. Sekatski, J.-D. Bancal, S. Wagner, and N. Sangouard, Phys. Rev. Lett. **121**, 180505 (2018).
[23] E. Schrödinger, Naturwissenschaften **23**, 807 (1935).
[24] E. E. Wollman, C. U. Lei, A. J. Weinstein, J. Suh, A. Kronwald, F. Marquardt, A. A. Clerk, and K. C. Schwab, Science **349**, 952 (2015).
[25] A. D. O'Connell *et al.*, Nature (London) **464**, 697 (2010).
[26] Y. Chu, P. Kharel, W. H. Renninger, L. D. Burkhart, L. Frunzio, P. T. Rakich, and R. J. Schoelkopf, Science **358**, 199 (2017).
[27] S. Hong, R. Riedinger, I. Marinković, A. Wallucks, S. G. Hofer, R. A. Norte, M. Aspelmeyer, and S. Gröblacher, Science **358**, 203 (2017).
[28] A. P. Reed *et al.*, Nat. Phys. **13**, 1163 (2017).
[29] T. Palomaki, J. Teufel, R. Simmonds, and K. Lehnert, Science **342**, 710 (2013).
[30] K. C. Lee *et al.*, Science **334**, 1253 (2011).
[31] R. Riedinger, A. Wallucks, I. Marinković, C. Löschnauer, M. Aspelmeyer, S. Hong, and S. Gröblacher, Nature (London) **556**, 473 (2018).
[32] C. F. Ockeloen-Korppi, E. Damskägg, J.-M. Pirkkalainen, M. Asjad, A. A. Clerk, F. Massel, M. J. Woolley, and M. A. Sillanpää, Nature (London) **556**, 478 (2018).
[33] S. J. van Enk, N. Lütkenhaus, and H. J. Kimble, Phys. Rev. A **75**, 052318 (2007).
[34] V. C. Vivoli, T. Barnea, C. Galland, and N. Sangouard, Phys. Rev. Lett. **116**, 070405 (2016).

[35] S. G. Hofer, K. W. Lehnert, and K. Hammerer, Phys. Rev. Lett. **116**, 070406 (2016).
[36] J. Chan, A. H. Safavi-Naeini, J. T. Hill, S. Meenehan, and O. Painter, Appl. Phys. Lett. **101**, 081115 (2012).
[37] See Supplemental Material at http://link.aps.org/supplemental/10.1103/PhysRevLett.121.220404 for additional information on the setup, measurement techniques and data analysis, which includes Ref. [38].
[38] J. Minář, H. de Riedmatten, C. Simon, H. Zbinden, and N. Gisin, Phys. Rev. A **77**, 052325 (2008).
[39] M. A. Horne, A. Shimony, and A. Zeilinger, Phys. Rev. Lett. **62**, 2209 (1989).
[40] R. Riedinger, S. Hong, R. A. Norte, J. A. Slater, J. Shang, A. G. Krause, V. Anant, M. Aspelmeyer, and S. Gröblacher, Nature (London) **530**, 313 (2016).
[41] H. de Riedmatten, J. Laurat, C. W. Chou, E. W. Schomburg, D. Felinto, and H. J. Kimble, Phys. Rev. Lett. **97**, 113603 (2006).
[42] B. S. Cirel'son, Lett. Math. Phys. **4**, 93 (1980).
[43] R. N. Patel, C. J. Sarabalis, W. Jiang, J. T. Hill, and A. H. Safavi-Naeini, Phys. Rev. Applied **8**, 041001 (2017).
[44] G. MacCabe, H. Ren, J. Luo, J. Cohen, H. Zhou, A. Ardizzi, and O. Painter, APS March Meeting, 2018.
[45] A. Bassi, K. Lochan, S. Satin, T. P. Singh, and H. Ulbricht, Rev. Mod. Phys. **85**, 471 (2013).
[46] S. Bose, A. Mazumdar, G. W. Morley, H. Ulbricht, M. Toroš, M. Paternostro, A. A. Geraci, P. F. Barker, M. S. Kim, and G. Milburn, Phys. Rev. Lett. **119**, 240401 (2017).
[47] C. Marletto and V. Vedral, Phys. Rev. Lett. **119**, 240402 (2017).